Reconstitution of the type-1 active site of the H145G/A variants of Nitrite Reductase by ligand insertion

Wijma, H.J.; Boulanger, M.J.; Molon, A.; Fittipaldi, M.; Huber, M.I.; Murphy, M.E.P.; ... ; Canters, G.W.

Reconstitution of the Type-1 Active Site of the H145G/A Variants of Nitrite Reductase by Ligand Insertion†

Hein J. Wijma,‡ Martin J. Boulanger,§ Annamaria Molon,‡ Maria Fittipaldi,⊥ Martina Huber,⊥ Michael E. P. Murphy,§,# Martin Ph. Verbeet,‡ and Gerard W. Canters*,‡

Gorlaeus Laboratories, Metallo Protein Group, Leiden University, P. O. Box 9502, 2300 RA Leiden, The Netherlands, Departments of Biochemistry and Molecular Biology and of Microbiology and Immunology, University of British Columbia, Vancouver, BC V6T 1Z3, Canada, and Department of Molecular Physics, Leiden University, P. O. Box 9504, 2300 RA Leiden, The Netherlands

Received December 2, 2002; Revised Manuscript Received January 30, 2003

ABSTRACT: Variants of the copper-containing nitrite reductase (NiR) of *Alcaligenes faecalis* S6 were constructed by site-directed mutagenesis, by which the C-terminal histidine ligand (His145) of the Cu in the type-1 site was replaced by an alanine or a glycine. The type-1 sites in the NiR variants as isolated, are in the reduced form, but can be oxidized in the presence of external ligands, like (substituted) imidazoles and chloride. The reduction potential of the type-1 site of NiR-H145A reconstituted with imidazole amounts to 505 mV vs NHE (20 °C, pH 7, 10 mM imidazole), while for the native type-1 site it amounts to 260 mV. XRD data on crystals of the reduced and oxidized NiR-H145A variant show that in the reduced type-1 site the metal is 3-coordinated, but in the oxidized form takes up a ligand from the solution. With the fourth (exogenous) ligand in place the type-1 site is able to accept electrons at about the same rate as the wt NiR, but it is unable to pass the electron onto the type-2 site, leading to loss of enzymatic activity. It is argued that the uptake of an electron by the mutated type-1 site is accompanied by a loss of the exogenous ligand and a concomitant rise of the redox potential. This rise effectively traps the electron in the type-1 site.

To convert nitrite (NO_2^-) into nitric oxide (NO) and water, the copper-containing nitrite reductases (NiRs)[1] from a variety of denitrifying bacteria use two copper sites: (A) a type-1 site to acquire reducing equivalents in the form of electrons from redox partner proteins, like pseudo-azurin in the case of *Alcaligenes faecalis* (*1*, *2*), and (B) a type-2 site to catalyze the enzymatic conversion (*3*−*5*). The 13-bond long covalent connection between the two Cu centers provides for sufficient electronic coupling to guarantee a rate of electron transfer from the type-1 to the type-2 center that is compatible with physiological needs.

We have modified the type-1 copper site of *A. faecalis* NiR by replacing the C-terminal ligand histidine of this site by a glycine or an alanine. The resulting gap in the first coordination shell of the Cu makes the metal accessible to external ligands; it provides a means to study the role of the type-1 site in the catalytic cycle and to establish the importance of this ligand for the functioning of the enzyme (*6*−*12*). A similar modification has been applied in the past to the much simpler blue copper protein azurin, where it was shown that this type of modification can be very revealing about the properties of Cu in a biological context.

The present work focuses on the construction, expression, and purification of the above-mentioned NiR variants, and on their structural and enzymatic characterization. In particular, the reconstitution of the type-1 site with external ligands is addressed in relation to the catalytic activity of the enzyme. Crystallographic data of H145A NiR with the type-1 site in the reduced and in the oxidized form provide a solid basis for interpreting the spectroscopic and kinetic results. It is the first time that the crystallographic structure of a type-1 site with this type of mutation is reported. The results show that various exogenous ligands can bind to the *oxidized* type-1 site and restore the spectroscopic features characteristic of these sites. On the other hand, the *reduced* type-1 site stays three-coordinate and does not bind exogenous ligands. Electron transfer to the oxidized type-1 sites in the NiR variants, provided exogenous ligands are bound, occurs at rates similar to the native NiR, but internal electron transfer from the reduced type-1 to the oxidized type-2 site does not occur in the variants irrespective of whether external ligands are present or not. Thus, the mutant NiRs exhibit

† This work is supported by a Research Grant from the National Science and Engineering of Research Council of Canada (M.E.P.M). M.J.B. and H.J.W. are supported by a University Graduate Fellowship, and M.E.P.M. is a Canadian Institutes of Health Research Scholar.

* Corresponding author: G. W. Canters, Phone: (31) 71 527 4256, Fax: (31) 71 527 4349, E-mail: canters@chem.leidenuniv.nl.

‡ Gorlaeus Laboratories, Leiden University.

§ Departments of Biochemistry and Molecular Biology, University of British Columbia.

Department of Microbiology and Immunology, University of British Columbia.

⊥ Department of Molecular Physics, Leiden University.

[1] Abbreviations: afNiR, copper-containing nitrite reductase of *Alcaligenes faecalis* S6; cyt c^{2+}, horse-heart ferrocytochrome *c*; E'_0, standard reduction potential; EPR, electron paramagnetic resonance; H117G-Im, H117G variant of *Pseudomonas aeruginosa* azurin with imidazole bound; H145A-Im, H145A variant of afNiR with imidazole bound; Mes, 2-(*N*-morpholino)ethane-sulfonic acid; Mops, 3-(*N*-morpholino)propanesulfonic acid; UV−Vis, UV and visible range; wt, wild type (native).

10.1021/bi027270+ CCC: $25.00
Published on Web 03/21/2003

impaired catalytic activity. The work reported here opens the road to possible hot wiring of NiR.

MATERIALS AND METHODS

Site-Directed Mutagenesis, Protein Expression, and Purification. For overexpression and mutagenesis a pET28a-based vector containing the wt NIR gene from *A. faecalis* S6 (*13*) was used (*14*). To replace the histidine at position 145 by PCR mutagenesis, the following oligo-nucleotides were used: NIR−H145G forward primer 5′-GCACCTCCCGGGATGGTTCCCTGG**GGT**GTCGTATCGGGC-3′ and NIR-H145G reverse primer 5′-GCCCGATACGAC**ACC**CCAGGGAACCATCCCGGGAGGTGC-3′. The mutated codon is in bold and the introduced Xma I restriction site is underlined. The NiR-H145A forward and reverse primers were identical to those used for the H145G mutation except that the mutated codons were GCT and AGC, respectively. The base-pair alterations were confirmed by DNA sequencing. The wt and mutant NiRs were overexpressed and purified essentially as described (*14*), except that the cells were precultured at 30 °C before induction with IPTG, and were subsequently cultured overnight at 25 °C. The lower temperatures increased the final yield to 200 mg of pure NiR per liter of culture. Further slight modifications of the procedure included the addition of $CuCl_2$ (100 μM) to the 2 YT medium, while during the lysis step 1 mM of $CuCl_2$ was added to ensure copper incorporation into the type-2 site. After the first column step, Tris buffer was used instead of phosphate buffer.

Preparation of H145G/A−Ligand Complex. NiR-H145G and -H145A complexed with imidazole were obtained by incubating the NiRs (20 μM) at 4 °C with a large excess of imidazole (10 mM, pH 7) to which $K_3Fe(CN)_6$ (300 μM) and $CuNO_3$ (100 μM) was added. After 16 h, the samples were centrifuged for 1 h at 5300 g; the supernatant was washed by ultrafiltration with 500 mM NaCl (buffered by 5 mM Mops, pH 7) to remove ferricyanide and aspecifically bound copper. The chloride was subsequently exchanged for other ligands by ultrafiltration with a buffered solution of the proper ligand (substituted imidazoles; concentration: 2 mM).

Assays. Protein concentrations were determined with the Bradford assay. In this way, an $\epsilon_{280\ nm}$ of 46 $mM^{-1}\ cm^{-1}$ per monomer was found for both wt and mutant NiRs. Copper contents were determined by the bicinchoninic acid method after complete reduction of the sample (*15*). This method, in our hands, gave better reproducible results than a determination by atomic absorption spectroscopy. The zinc content was determined by atomic absorption spectroscopy with the use of internal standards. Electron-spray mass spectrometry was performed at the mass spectroscopy center of the Medical Faculty in Leiden (LUMC, The Netherlands). Activity assays using methyl viologen-dithionite as the electron donating couple were performed according to ref *1*. One unit of activity is defined as catalyzing the conversion of 1 μmol of nitrite/min. For stopped-flow measurements an Applied Photophysics SX18MV instrument was used. Preparation of the stopped-flow machine for anaerobic experiments and sample handling was according to the protocol supplied by Applied Photophysics that recommends the glucose oxidase-catalase system (*16*) for flushing of the tubing and the reaction chamber prior to experiments. Cyclic voltammetry (CV) of wt afNiR was performed at room temperature as described elsewhere (*17*) in the presence of apo-pseudoazurin of *A. faecalis* in 100 mM of potassium phosphate, pH 7.

Spectroscopy. Electronic spectra were recorded on a Perkin-Elmer Lambda 800. To minimize light scattering, samples were first spun for 10′ at 16 000 g, at 4 °C to remove aggregated protein. The X-band EPR measurements were carried out using an Elexsys X-band Bruker spectrometer with a rectangular cavity. The measurements were performed at 40 K using an Oxford helium cryostat ESR 900.

Crystal Structure Determination. Crystals of NiR-H145A were grown at room temperature in mother liquor consisting of 0.1 M sodium cacodylate, pH 5.5, 0.1 M sodium acetate, pH 4.7, 2 mM zinc acetate, 2 mM copper chloride, pH 5.5 and 8 to 12% poly(ethylene glycol) 6000. These conditions resulted in crystals that grew in an orthorhombic lattice (space group $P2_12_12_1$). For the imidazole reconstituted H145A structure, the mother liquor was supplemented with 10 mM imidazole and 2 mM $CuCl_2$. The NiR concentration used was 10 to 15 mg/mL. Prior to freezing in a nitrogen stream, crystals were incubated for 1 min in mother liquor with 30% glycerol as a cryoprotectant. Crystals were looped directly into a cryostream at 100 K generated by a cryostat (Oxford Cryo Systems, Oxford, U.K.). X-ray data were collected on a Rigaku R-AXIS IIc image plate system with CuKα radiation generated by a Rigaku RU 300 rotating anode operating at 100 mA and 50 kV and focused with Osmic confocal max-flux optical mirrors. All data sets were collected to at least 1.9 Å resolution and processed with DENZO (*18*).

The H145A crystals contain the assembled NiR trimer in the asymmetric unit. The structure of nitrite-soaked wt NiR (*19*) was used as the starting model for the native H145A structure following removal of the His145 side-chain, nitrite, and all the solvent atoms. The H145A variant structure was subsequently used as the starting model for the imidazole-reconstituted H145A structure. The final structure of each mutant begins at Ala4 and ends at Glu339. Five percent of the data were set aside for calculation of the free R-factor (*20*). Standard CNS (*21*) maximum likelihood positional and B-refinement was carried out with solvent being added with the WATERPICK procedure. The copper ligand geometry and the positions of the copper and chloride ions were not restrained throughout the refinement. The R_{work} and R_{free} refinement statistics were calculated to be less than 20 and 23%, respectively, in both structures. Over 90% of the residues in each structure occupy the most favorable position in the Ramachandran plot as described by PROCHECK (*22*, *23*). Statistics of data processing and structure refinement are presented in Table 1.

RESULTS

NiR−H145G/A with Reduced Type-1 Site. The *optical spectrum* of the green colored solution of the purified wild type (wt) NiR agreed with published data (*1*) (Figure 1A). By contrast, the optical spectra of the colorless NiR-H145G and -H145A protein solutions showed no features in the visible range except for a weak absorption at 790 nm (Figure 1A), which disappeared upon incubation with dithionite. The

Table 1: Crystallographic Data Collection and Refinement Statistics

	H145A	H145A-Cl
crystal		
cell dimensions (Å)	$a = 61.60$	$a = 61.80$
	$b = 102.5$	$b = 102.5$
	$c = 146.0$	$c = 146.0$
resolution (Å)	1.90 (2.05−1.90)[a]	1.80 (1.91−1.80)
R-merge	0.088 (0.261)	0.041 (0.141)
$\{I\}/\{\sigma(I)\}$[b]	13.6 (4.65)	26.4 (7.38)
completeness (%)	87.6 (86.0)	90.0 (68.0)
unique reflections	64626 (12511)	78136 (9687)
working R-factor	0.174	0.156
free R-factor	0.225	0.195
rmsd bond length (Å)	0.009	0.011
overall B-factor (Å^2)[c]	24.6	16.2
water molecules	1251	1346
PDB entry code	1NPJ	1NPN
	RCSB018084	RCSB018085

[a] Values in parentheses are for the highest resolution shell. [b] $\{I\}/\{\sigma(I)\}$ is the average intensity divided by the average estimated error in intensity. [c] B-factors are an average from all three monomers.

experimentally determined *masses* of the NiRs were in good agreement with the calculated masses (Table 2). *Metal content* determinations showed that all purified NiRs were fully loaded with copper (Table 2); no zinc could be detected. In the *EPR-spectra* of wt NiR the signals of both the type-1 site and the type-2 site could be distinguished in accordance with literature data (*24*) (Figure 2); only signals of the type-2 site were observed in the EPR spectra of the NiR H145G and H145A variants. Since the copper content of the purified NiR variants is consistent with full occupation of both sites, the absence of UV−Vis absorption bands and of a type-1 EPR absorption signal means that the type-1 site in NiR H145G/A was reduced and consequently spectroscopically silent.

Oxidation of the NiR H145G/A Type-1 Site. It appeared impossible to oxidize the type-1 sites of NiR H145G and NiR H145A by treatment with $Fe(CN)_6^{3-}$ or $IrCl_6^{2-}$. However, in the presence of 10 mM imidazole, addition of $Fe(CN)_6^{3-}$ resulted in the slow appearance of an absorption around 590 nm, typical of an oxidized type-1 site. Apparently, the imidazole acts as an external ligand for this site. Oxidation of the type-1 site could also be observed by using $IrCl_6^{2-}$ in the presence of 500 mM NaCl in which case chloride acts as the external ligand (vide infra; see also ref *12*). External ligands (chloride, substituted imidazoles) could be exchanged for each other by ultrafiltration. To confirm the presence of oxidized type-1 Cu sites, EPR spectra were recorded. In the spectra of imidazole reconstituted oxidized NiR-H145G/A (NiR H145G/A-Im) signals of the type-1 site are present as well as those of the type-2 site (Figure 2).

The preparation of oxidized, imidazole-reconstituted H145G/A-Im as described in Materials and Methods resulted in protein in which about 50% of the type-1 sites was oxidized as demonstrated by the further increase of the 590 nm absorption upon addition of fresh $Fe(CN)_6^{3-}$. Extinction coefficients were determined from titration of the partly oxidized NiRs with reduced horse-heart cytochrome *c* (Table 3).

The reduction potential of wt afNiR as measured by cyclic voltammetry at room-temperature amounted to 260 mV versus NHE. The redox potential of NiR-H145A in the presence of imidazole was determined by incubation overnight in a ferri/ferrocyanide redox buffer and determination of the degree of oxidation of the type-1 site afterward by measuring the optical extinction at 593 nm; it amounted to 505 mV in the presence of 10 mM imidazole at pH 7 (see Figure 3).

The use of buffers such as Mops/Mes and phosphate, at medium to high concentrations (50−500 mM), gave rise to optical absorbances in the visible region for oxidized NiR variants, suggesting binding of buffer components. Therefore, buffer concentrations were kept as low as possible, usually below 10 mM, to minimize interference in the ligand binding experiments. In an attempt to observe the spectrum of the oxidized type-1 site in the absence of external ligands, oxidized enzyme was prepared first in the presence of an external ligand after which the ligand was removed as quickly as possible (within 1 h) by extensive ultrafiltration against buffer at very low buffer concentrations (2 mM Mops, pH 6.5, 4 °C). This yielded protein preparations with a unique optical spectrum, the intensity of which slowly decreased with time (Figure 4). Treating the bleached solution with ferricyanide and imidazole restored the absorbance around 590 nm, indicating that the bleaching was due to autoreduction of the type-1 site.

Enzymatic Activity. For NiR-H145G/A the enzymatic activity in the conversion of nitrite was 2 orders of magnitude less than that of wt NiR (see Table 2). The presence of imidazole made no difference. To probe the origin of this low enzymatic activity, the electron transfer to the type-1 site was studied by stopped-flow experiments. As an electron donor cytochrome c^{2+} was chosen. Cytochromes are commonly applied in the study of the ET kinetics with NiR. They have the advantage over blue copper proteins such as pseudoazurin, of possessing an improved sensitivity due to their high differential absorbance. On mixing of oxidized wt NiR with excess cyt c^{2+} (*25*−*27*), a burst in cyt c^{2+} consumption was observed that decreased exponentially in time (Figure 5). When excess nitrite was present, the burst continued until all cyt c^{2+} had been oxidized. Upon mixing H145G/A-Im with cyt c^{2+} an exponential decrease of cyt c^{2+} was also observed, but the addition of nitrite had no effect either on the rate of cyt c^{2+} consumption or on the total amount of cyt c^{2+} consumed. Reduced NiR-H145G/A (type-1 site in the Cu^I state) did not oxidize cyt c^{2+}, neither in the presence nor the absence of nitrite. With substituted imidazoles (1-methylimidazole, 4-methylimidazole) instead of imidazole similar observations were obtained. An overview of the kinetic data is presented in Table 4.

Crystallographic Results. We succeeded in crystallizing NiR-H145A (type-1 site reduced; see Figure 6A) and NiR H145A-Cl (type-1 site oxidized; see Figure 6B). Overall, there is little change in the fold of the H145A variant structures relative to the native NiR structure as revealed by a root-mean-squared deviation between the Cα chains of less than 0.2 Å. The substitution of a histidine with an alanine at the type-1 site does not seem to affect the occupation of the type-2 copper sites, which appear fully occupied based on a comparison of the B-values of the metal and the ligands and the electron density peak heights. The main structural differences between the H145A variant and the native enzyme are localized at the type-1 copper site.

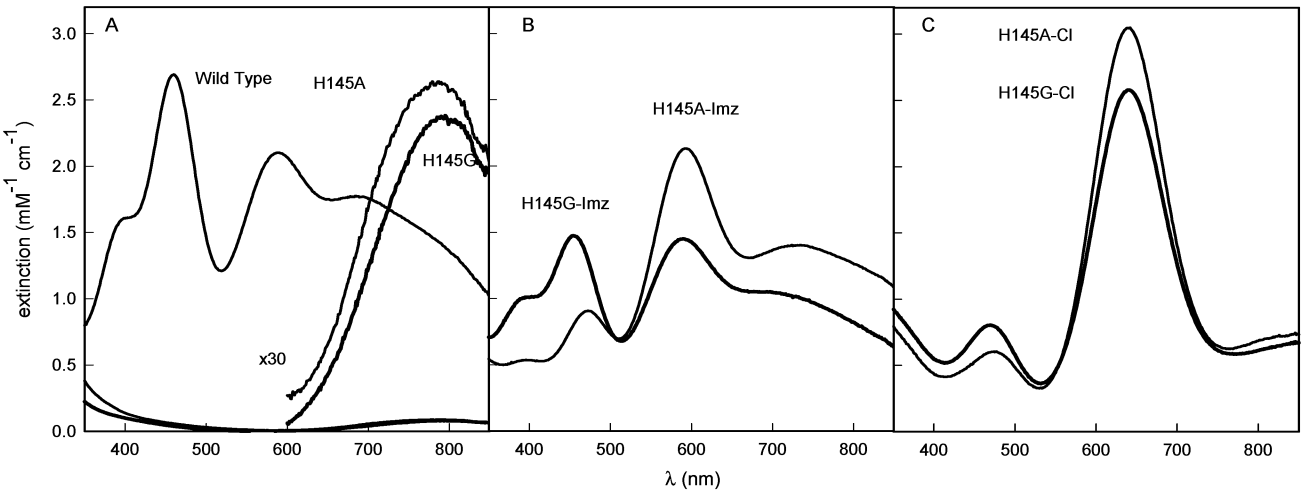

FIGURE 1: Optical spectra of native NiR and derivatives. To minimize light scattering, all samples were spun for 10 min (16000*g*, at 4 °C) to remove aggregated protein. The vertical axis in all spectra is scaled to a concentration of 1 mM of NiR **(**A) Native NiR (WT) and NiR H145G/A in 20 mM Mops pH 7.0; (B) NiR H145G/A reconstituted with imidazole. Recorded in 2 mM imidazole pH 7.0; (C) NiR H145G/A after exchange of imidazole with chloride (500 mM in 5 mM Mops, pH 7.0).

Table 2: Physical Characteristics of the Purified Nitrite Reductases

	wild type	H145G	H145A
activity (units/mg)	550 ± 50	8.9 ± 2.0	4.7 ± 1.0
Cu-content per monomer[a]	2.0	2.0	1.9
measured mass (D)	36.838 ± 4	36.758 ± 4	36.771 ± 4
calculated mass (D)	36.838	36.758	36.772

[a] Reproducibility better than 5%.

Oxidized NiR-H145A. In the structure of the H145A variant, the side-chain of residue 145 is nearly 3.6 Å shorter than that of the histidine in the native structure resulting in a channel between the copper atom and the bulk solvent. In the structure an exogenous ligand is present. Although the starting material was H145A-Im, the electron density strongly suggests that the ligand is a chloride (Figure 6B). Chloride was present in the crystallization buffer in a final concentration of 2 mM. Furthermore, the vivid blue color of the crystals differed from that of the blue-green starting solution of NiR H145A-Im, but it was similar to that of a solution of H145A-Cl. Refinement of the structure resulted in a distance of the chloride to the copper of 2.29 Å which, within experimental error, is identical to the Cu−Cl distance in azurin H117G-Cl (2.22 Å) as measured by EXAFS (*28*).

The coordination of the chloride-reconstituted type-1 site is similar to the site in the wt protein in that it is tetrahedral, although it is not identical to the native site (Table 5). Relative to the position of the coordinating Nδ1 atom of the His145 side-chain in the native structure, the exogenous chloride ligand is shifted approximately 1.32 Å toward the side-chain of Met62 (not a Cu-ligand) (Figure 6B). As a result, Met62 adopts a new conformation where the χ_2 angle is changed by nearly 120° accompanied by a shift of the Sδ atom of approximately 2.4 Å away from the type-1 copper when compared to to the native structures (reduced and oxidized type-1 site) and the H145A structure (type-1 site reduced). The mutation at position 145 and the reorientation of the Met62 side-chain in the chloride-reconstituted structure represent the only significant structural differences from the native structure (*19*). The remaining metal−ligand distances did not differ significantly from the native structure.

Reduced NiR-H145A. In reduced NiR-H145A, there is no electron density of an exogenous ligand present (see Figure 6A). The Cu atom in the type-1 site is coordinated trigonally by the Sγ of Cys136, the S$_\delta$ of Met150 and the N$_\delta$ of His95. Furthermore, the distance of the Cu atom to the plane of these remaining type-1 site ligands has decreased in H145A to 0.27 Å as compared to H145A-Cl (0.57 Å) and native NiR (0.64 Å) (Table 5). These differences are significant as indicated by the range calculated from comparing the different type-1 sites in the asymmetric unit. Thus, for the reduced site the coordination is significantly different from that of wt. In particular, no exogenous ligand is bound and the Cu(I) is tricoordinated by the remaining ligands.

DISCUSSION

Spectroscopic and Structural Features. The H145A and H145G mutations lead to stable NiR variants with fully occupied type-1 and type-2 sites. In the proteins, as isolated, the type-1 site is reduced, while the type-2 site is oxidized (see the EPR spectrum, Figure 2, traces B and C). The optical spectrum of the NiR-145G/A variants is featureless except for a weak absorption around 790 nm (see Figure 1A; $\epsilon_{790} = 85 \pm 10$ M^{-1} cm^{-1}), which disappears upon incubation with dithionite. We ascribe this absorption to the oxidized type-2 site and its disappearance to reduction of the site. Similar absorption bands have been observed for a variant of NiR containing spectroscopically silent zinc in the type-1 site (*24*), and for type-2 sites in copper containing oxidoreductases (500 nm < λ_{max} < 1 μm; ϵ_{max} < 200 M^{-1} cm^{-1}) (*29*).

Commonly used oxidants such as $Fe(CN)_6^{3-}$ or $IrCl_6^{2-}$ can oxidize the type-1 site only in the presence of a large excess of external ligands, like (substituted) imidazoles or chloride. Such a behavior has also been observed for the His117Gly variant of azurin from *Pseudomonas aeruginosa*. In azurin, His117 occupies a similar position as His145 in the 3D structure of NiR. For the azurin variant it was found that the type-1 Cu site is three-coordinated in the reduced form, while in the oxidized form the Cu has a strong preference for a four-coordination, the fourth ligand coming from the solution. In the absence of external ligands the Cu-

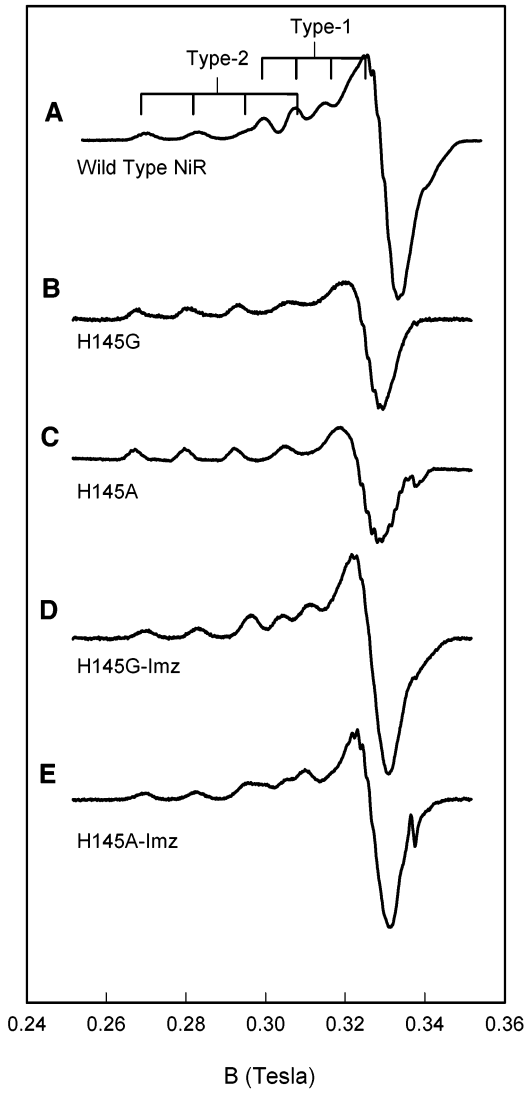

FIGURE 2: X-band EPR spectra of native NiR and derivatives. (A) native NiR; (B) H145G as isolated; (C) H145A as isolated; (D) H145G reconstituted with imidazole; (E) H145A reconstituted with imidazole. Modulation amplitude: 0.5 mT; modulation frequency: 100 kHz; microwave power: 0.6 mW; total measurement time: 21 min per run. Enzyme samples (150−300 μM) were prepared in 30−40% glycerol. Measurements were carried out at 40 K using an Elexsys X-band Bruker spectrometer with a rectangular cavity. The signal around 340 mT is ascribed to a small contamination.

Table 3: Wave Lengths of Absorption Maxima λ_{Max} (nm) and Extinction Coefficients ϵ (cm^{-1} mM^{-1}) in the Optical Spectra of Wild Type and Imidazole Reconstituted H145G/A

nitrite reductase	λ_{max} (nm)/ϵ (cm^{-1} mM^{-1})[a]			
wild type		460 / 2.9	589 / 2.2	685 / 1.9
H145G-Im		454 / 2.9	589 / 2.9	
H145G-1-methyl-Im	385 / 2.3	459 / 3.1	594 / 3.4	
H145G-4-methyl-Im	380 / 2.0	457 / 2.6	597 / 3.1	
H145A-Im		472 / 1.3	593 / 3.5	735 / 2.3
H145A-1-methyl-Im		477 / 1.2	599 / 4.7	
H145A-4-methyl-Im		474 / 1.9	594 / 3.7	726 / 2.8

[a] Extinction coefficients were determined by titrating a (partially) oxidized solution of NiR with horse-heart cyt c^{2+} and using a $\Delta\epsilon_{550\ nm}$ = 21.2 mM^{-1} cm^{-1} for calculating the concentration of oxidized NiR. Accuracy of quoted values: ± 5%

(II) form is destabilized with respect to the Cu(I) form which gives rise to a strong increase in redox potential (up to 670 mV in the case of *P.a.* H117G azurin). On the other hand,

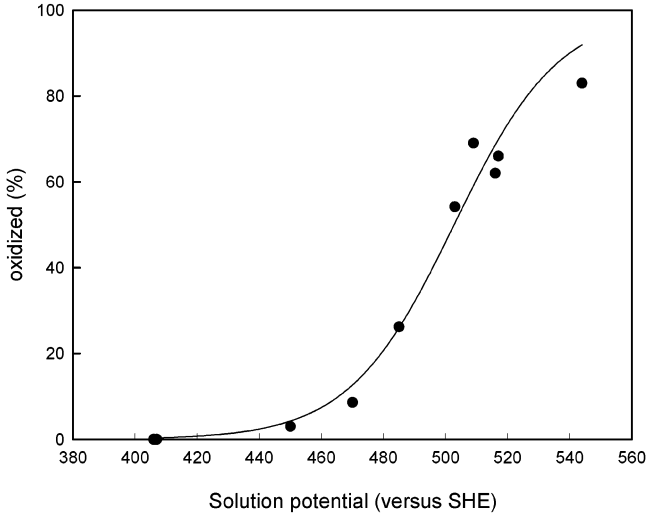

FIGURE 3: Reduction-potential of H145A-Imz. NiR H145A (10 μM) was incubated anaerobically overnight in a solution containing 10 mM of imidazole, 100 μM of $CuNO_3$, and a 300 μM mixture of ferri/ferrocyanide. After incubation of the sample, the redox-potential of the solution was measured using a calomel electrode and the absorbance at 593 nm was determined. The percentage of oxidized protein was determined using the extinction coefficients reported in Table 3. The data were fitted to the Nernst equation to obtain a value for the redox potential.

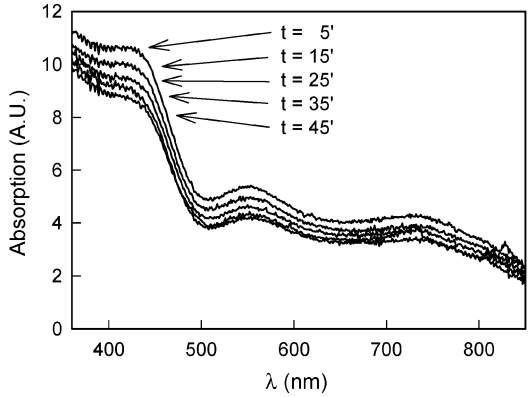

FIGURE 4: Decrease (after removal of exogenous ligands) in absorbance of oxidized NiR-H1145G over time in 2 mM Mops at pH 6.5 at 15 °C. Spectra were recorded at 10 min intervals, starting 5 min after diluting a sample from a 200 mM of MOPs pH 6.5 solution one hundred times with demineralized water.

at very high concentrations of an external ligand the redox potential drops to values that are common for blue copper proteins (260 mV for H117G azurin when extrapolated to infinite Imz concentration). This dependence of the redox potential on external ligand concentration is intimately connected with a dependence of the dissociation constant of the external ligand on the redox state of the copper (K_d^{app} increases from 3.6 μM to 14 M upon reduction of the azurin H117G at pH 6 (*12*)).

For the NiR-145G/A variants, a similar behavior is observed: the ox-form of the type-1 site is stable only in the presence of external ligands; otherwise it becomes reduced through autoreduction. In the presence of 10 mM imidazole the reduction potential of NiR-H145A is 250 mV higher than that of the native enzyme. This change in potential indicates a difference in affinity for external ligands between the oxidized and reduced state similar to that observed in H117G azurin.

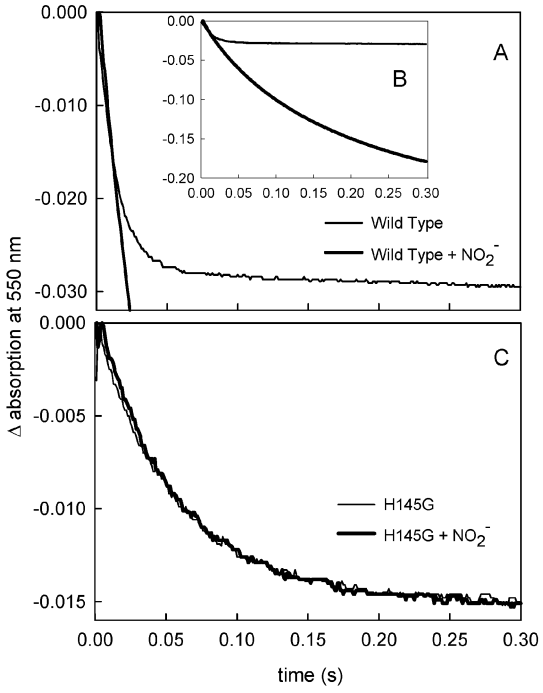

FIGURE 5: Pre-steady-state ferrocytochrome *c* consumption by NiR. Samples were mixed under anaerobic conditions as reported in Materials and Methods. (A) Decrease in absorption at 550 nm upon mixing wt NIR (1 μM) with cyt c^{2+} (10 μM); (B) As A but displayed on a larger scale, (C) H145G-Im (0.94 μM) with cyt c^{2+} (15 μM).

Table 4: Pre-Steady-State cyt c^{2+} Consumption by NiR WT and Imidazole Reconstituted H145G/A[a]

nitrite reductase	second order rate constants (10^6 M^{-1} s^{-1})[b]
wild type	6.5
H145G-Im	2.0
H145G-1-methylimidazole	0.75
H145G-4-methylimidazole	0.70
H145A-Im	4.0
H145A-1-methylimidazole	4.5
H145A-4-methylimidazole	0.95

[a] Conditions: 20 °C in 2 mM of either imidazole or a substituted imidazole buffered anaerobic solution at pH 7. [b] Second order rate constants (k_2) were calculated by dividing k_{obs} by [cyt c^{2+}] ($k_{obs} = k_2$[cyt c^{2+}]) and are based on three assays. Accuracy: ± 20%.

Crystallographic evidence indeed shows that the copper in the type-1 site, when reduced, is three-coordinate with a relatively short Cu−Sδ bond, while the metal is pulled toward the plane of the three ligands (His50−Nδ, Cys143−Sγ, His146−Nδ). This is reminiscent of what has been reported for the structure of the active site of reduced plastocyanin at low pH (*30*, *31*). For the oxidized type-1 site the crystallographic evidence shows that the Cu-site is four-coordinate, the fourth ligand being a chloride in the present case.

The optical data can also be combined with the crystallographic data to check the purported relation (*32*, *33*) between the intensity ratio of the 450 and 600 nm bands in the optical spectrum of a type-1 site and the value of the dihedral angle, θ, between the S(Met)−Cu−S(Cys) plane and the plane containing the N(His)−Cu−fourth ligand as illustrated in Figure 7. It appears that the points corresponding with the type-1 site in wt and H145A-Cl NiR fit the correlation line very well. Remarkably, in the case of NiR-145G/A the value of θ varies and allows for both blue and green NiR variants, depending on the external ligand (chloride vs imidazole, respectively). For H117G azurin these ligands only produced blue sites. Thus, in NiR, residue Met62 and possibly other elements of the structure around His145 are more flexible than the analogous region around His117 in azurin.

Kinetics. In the absence of external ligands the NiR-145A/G variants exhibit a residual enzymatic activity which is 2 orders of magnitude less than the activity of wt NiR. A similar low enzymatic activity (up to 5% of the wt) (*24*) has been observed for a NiR variant containing the redox-inactive zinc in its type-1 site (*47*). The type-1 site being disfunctional, this residual activity is ascribed to direct electron donation to the type-2 site by the dithionite/methyl viologen used in the nitrite reductase assay.

To investigate the electron transfer (ET) properties of the type-1 site, cytochrome c^{2+}, which reacts with the type-1 but not with the type-2 site of wt NiR, was used as a reductant. In the absence of nitrite, oxidized wt as well as the oxidized Imz-substituted H145A/G NiR variants exhibited single turn-over kinetics with similar rates (Table 4). Obviously, the mutations do not impede the type-1 site from acting as an electron acceptor. When repeating the assay in the presence of nitrite, however, a clear difference shows up between the wt NiR and the variants. The wt enzyme converts the nitrite until the source of reducing equivalents (i.e., the cytochrome c^{2+}) is exhausted, while the NiR-H145A/G variants do not show any enzymatic turnover. Clearly, the type-1 site in the NiR variants is able to accept an electron from an external donor when a strong external ligand for the Cu(II) is present, but fails to give the electron off to the type-2 site (i.e., to the site where the catalytic conversion occurs).

The explanation in light of the preceding data is that as soon as the type-1 site in the NiR variants is reduced, the Cu reverts to its three-coordinate form which is accompanied by a rise in redox potential of the type-1 site. This makes it impossible for the electron to move to the type-2 site, as the redox potential of the latter site is now below that of the type-1 site. Enzymatic activity would be possible only if the electron were transferred to the type-2 site before dissociation of the ligand from the type-1 site. Cyclic voltammetry experiments on protein films of H117G azurin have shown that the time constants of the dissociation and electrochemical steps are critical in deciding if a particular redox event may occur or not. In the present case dissociation of the external ligand from the reduced type-1 site in the NiR variants must be faster than the time needed for internal ET to the type-2 site (320−2000 s^{-1} (*48*−*50*)) and subsequent conversion of the nitrite.

Like in azurin (*28*) the covalent link between the imidazole ring (of histidine 145) and the protein scaffold of NiR seems essential for the surface-exposed histidine to bind both to the oxidized and the reduced type-1 copper. In the noncovalently associated imidazoles the entropic term of the Gibb's free energy increases dramatically when the bond to the copper is broken and the imidazole diffuses away. This shifts the equilibrium to unbound imidazole in the case of Cu^{1+}. For the native enzyme this dissociation step is not possible.

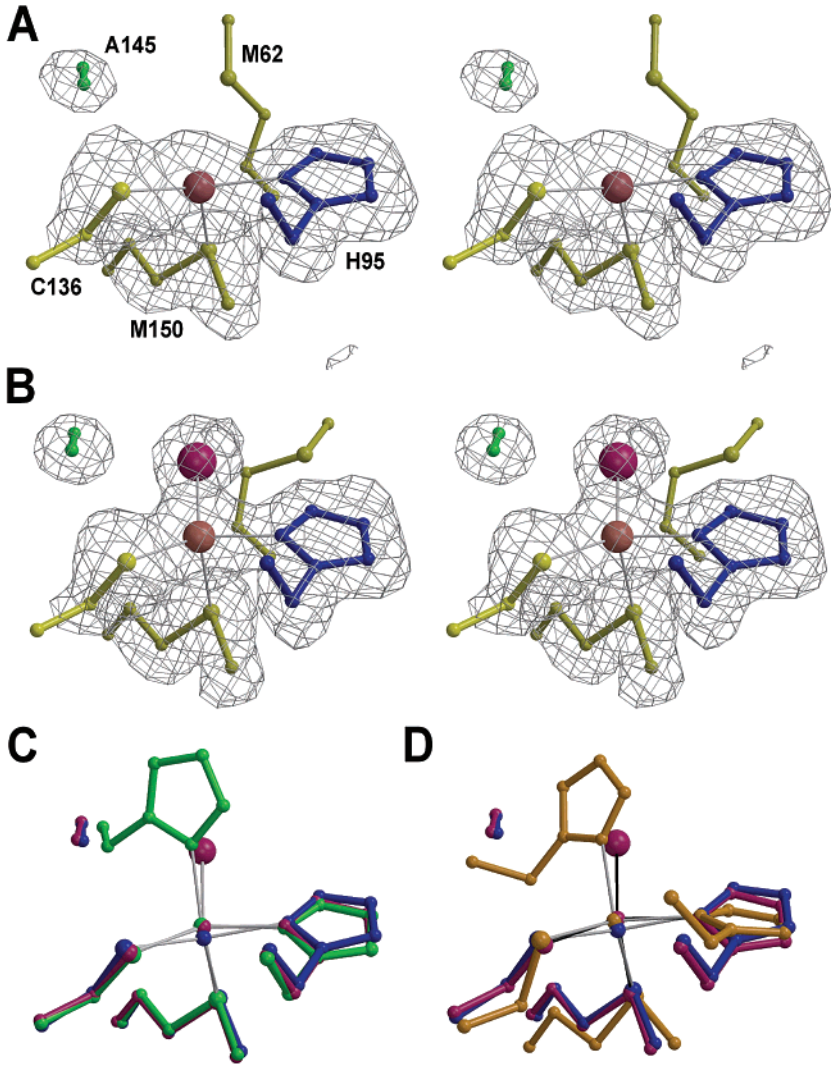

FIGURE 6: Stereoviews of the H145A NiR type-1 site in the (A) reduced and (B) oxidized state. (A) The side-chains and Cα atoms of residues 62, 95, 136, 145, and 150 are depicted as balls and sticks and are labeled. The copper atom is represented as a sphere. An omit difference electron density map of the ligand side chains and the copper atom is contoured at 4σ. In panel B, a chloride ion is included in the difference omit map (3.5σ) and is drawn as a large sphere above the copper. In panel C, the two structures are superimposed with the native NiR structure [entry code 2AFN, (*19*)]. Oxidized H145A is in magenta, reduced H145A is in blue, native NiR is green. In panel D, the H145A structures are superimposed with the oxidized plastocyanin structure in orange [entry code 5PCY, (*30*)].

SUMMARY AND OUTLOOK

Small blue copper proteins function as electron carriers in the cell. A distinguishing feature in their structures is the C-terminal copper ligand, a histidine that cuts through the so-called hydrophobic patch of the protein surface. It plays a crucial mechanistic role in that it provides for the electronic coupling between the redox center (Cu) and the redox partner (often another redox protein) required for efficient ET. When replacing this histidine by a small noncoordinating residue (like Gly or Ala) the ligand shell of the Cu changes from four- to three-coordinate thereby considerably stabilizing the Cu(I) over the Cu(II) state. One of the results is a substantial rise in redox potential.

In the present case, we have studied a similar modification applied to a redox *enzyme*, nitrite reductase, where the type-1 site mediates the shuttling of reducing equivalents between an outside redox partner and the site of catalysis, a type-2 Cu site. This provides the possibility to study the activity of the type-1 site by monitoring the enzymatic activity of the protein. The replacement of the C-terminal histidine ligand also in this case leads to a rise in redox potential, which, in the presence of suitable external ligands, can be partially reverted depending on binding strength and concentration of the ligand. Thus, the redox potential becomes dependent on the nature and the concentration of the ligand. The results of the present study can now be summarized as follows.

For the first time, solid crystallographic evidence has been obtained showing that the Cu in a mutated type-1 Cu site (C-terminal His into Gly/Ala) becomes three-coordinate when reduced. This is important corroboration of a conclusion that was based until now only on circumstantial, albeit extensive, evidence.

Further, the type-1 site in the NiR variants is still able to accept electrons in the presence of external ligands but is unable to pass the electron on to the catalytic site, presumably because the reduced type-1 site converts to the three-coordinate form and traps the electron. This opens up the possibility of kinetic control over the enzymatic activity. While the enzyme can still be loaded with reductive equivalents the transfer to the catalytic center depends on

Table 5: Metal Ligand Geometry of Type-1 Sites in wt Nitrite Reductase and the Oxidized and Reduced NiR-H145A[a]

	native afNiR	H145A T1 Cu^{1+}	H145A T1 Cu^{2+}
	Distances (Å)		
150 − Cu	2.62	2.54	2.66
95 − Cu	2.08	2.11	2.04
136 − Cu	2.13	2.17	2.19
145 − Cu	1.99	n/a	n/a
Cl − Cu	n/a[d]	n/a	2.29
Cu − NSS* distance[b]	0.64	0.27	0.57
	Angles (°)		
136−Cu−95	132	146	136
136−Cu−150	103	114	106
150−Cu−95	85	94	92
150−Cu−145	132	n/a	n/a
150−Cu−Cl	n/a	n/a	101
Θ[c]	64	n/a	83

[a] The numbers 95, 136, 145, and 150 in the left column refer to the N_δ of His95, the S_γ of Cys136, the N_δ of His145, and the S_δ of Met150. Sigma values (standard deviations determined from average values of three monomers in the asymmetric unit) amount to less than 3% for bond angles and less than 4% for bond distances. [b] This is the distance between the Cu atom and the NSS*-plane determined by the ligand atoms of residues His95/Cys136/Met150. [c] Θ is the dihedral angle between the planes through Cu−136−150 and the plane through Cu−136−145/Cl. [d] n/a: not applicable.

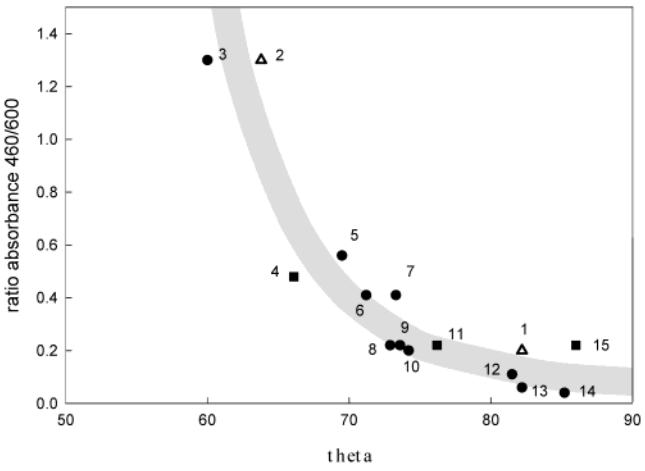

FIGURE 7: Relation between ratio of the absorbances at 460 and 600 nm versus dihedral angle θ. △: NiR from *A. faecalis*, ■: mutant proteins, ●: native proteins. A gray line was added as a visual aid. 1, AfNiR H145A-Cl; 2, AfNiR (*19*); 3, *A. cycloclastes* NiR (*34*); 4, *P. aeruginosa* M121H (*35*); 5, *N. gonorrheae* NiR (*36*); 6, cucumber basic blue protein (*37*); 7, *A. faecalis* pseudo-azurin (*38*); 8, *A. xylosidans* NiR (*39*); 9, *A. xylosidans* GIFU1051 NiR (*40*); 10, *Chloroflexus aurantacus* auracyanin (*41*); 11, *P. aeruginosa* M121E (*42*); 12, *P. versutus* amicyanin (*43*); 13, *Populus nigra* plastocyanin (*44*); 14, *P. aeruginosa* azurin (*45*); 15, *P. aeruginosa* M121Q (*46*).

the presence of an external ligand. By regulating the (effective) concentration of the ligand control may be exerted over the enzyme activity. This can be understood either in thermodynamic or in kinetic terms. Increasing the ligand concentration will lower the redox potential of the type-1 with respect to the type-2 site, thus increasing the probability of ET from one to the other site. Alternatively, an increase in ligand concentration can be seen as increasing the fraction of time the reduced type-1 site spends in the four-coordinate form, leading to enhanced ET to the type-2 site. Experiments on this subject are in progress.

The His to Gly/Ala mutation of a type-1 Cu site has been cited in the past as a construct that might allow wiring a type-1 site to a surface by applying an organic linker ("hot wire") that would terminate at one end into an imidazole group. The present experiments make it clear that this type of construct can also be applied to multicenter proteins and enzymes, provided attention is paid to enhance the local (effective) concentration of the ligand to the type-1 Cu.

REFERENCES

1. Kakutani, T., Watanabe, H., Arima, K., and Beppu, T. (1981) *J. Biochem. (Tokyo) 89*, 453−461.
2. Kakutani, T., Watanabe, H., Arima, K., and Beppu, T. (1981) *J. Biochem. (Tokyo) 89*, 463−472.
3. Libby, E., and Averill, B. A. (1992) *Biochem. Biophys. Res. Commun. 187*, 1529−1535.
4. Suzuki, S., Kataoke, K., Yamaguchi, K, Inoue, T., and Kai, Y. (1999) *Coord. Chem. Rev. 190*−*192*, 245−265.
5. Adman, E. T., and Murphy, M. E. P. (2001) in *Handbook of Metalloproteins* (Messerschmidt, A., Huber, R., Poulos, T., Wieghardt, K., Eds.) pp 1381−1390, John Wiley & Sons, Ltd, Chicester.
6. Den Blaauwen, T., Van de Kamp, M., and Canters, G. W. (1991) *J. Am. Chem. Soc. 113*, 5050−5052.
7. Barrick, D. (1995) *Curr. Opin. Biotechnol. 6*, 411−418.
8. van Pouderoyen, G., Andrew, C. R., Loehr, T. M., SandersLoehr, J., Mazumdar, S., Allen, H., Hill, H. A. O., and Canters, G. W. (1996) *Biochemistry 35*, 1397−1407.
9. Bonander, N., Karlsson, B. G., and Vanngard, T. (1996) *Biochemistry 35*, 2429−2436.
10. Farver, O., Jeuken, L. J. C., Canters, G. W., and Pecht, I. (2000) *Eur. J. Biochem. 267*, 3123−3129.
11. Gorren, A. C., den Blaauwen, T., Canters, G. W., Hopper, D. J., and Duine, J. A. (1996) *FEBS Lett. 381*, 140−142.
12. Jeuken, L. J. C., van Vliet, P., Verbeet, M. P., Camba, R., McEvoy, J. P., Armstrong, F. K., and Canters, G. W. (2000) *J. Am. Chem. Soc. 122*, 12186−12194.
13. Nishiyama, M., Suzuki, J., Kukimoto, M., Ohnuki, T., Horinouchi, S., and Beppu, T. (1993) *J. Gen. Microbiol. 139*, 725−733.
14. Boulanger, M. J., Kukimoto, M., Nishiyama, M., Horinouchi, S., and Murphy, M. E. (2000) *J. Biol. Chem. 275*, 23957−23964.
15. Brenner, A. J., and Harris, E. D. (1995) *Anal. Biochem. 226*, 80−84.
16. Englander, S. W., Calhoun, D. B., and Englander, J. J. (1987) *Anal. Biochem. 161*, 300−306.
17. Kohzuma, T., Shidara, S., and Suzuki, S. (1994) *Bull. Chem. Soc. Jpn. 67*, 138−143.
18. Otwinowski, Z. M., W. (1997) *Methods Enzymol. 276*, 307−326.
19. Murphy, M. E., Turley, S., and Adman, E. T. (1997) *J. Biol. Chem. 272*, 28455−28460.
20. Brunger, A. T. (1997) *Methods Enzymol. 277*, 366−404.
21. Brunger, A. T., Adams, P. D., Clore, G. M., Delano, W. L., Gros, P., R. W., G.-K., Jiang, J. S., Kuszewski, J., Nilges, N., Pannu, N. S., Rice, L. M., Simonson, T., and G. L., W. (1998) *Acta Crystallogr. 54*, 905−921.
22. Laskowski, R. A., MacArthur, M. W., Moss, D. S., and Thornton, J. M. (1993) *J. Appl. Crystallogr. 26*, 283−291.
23. Jones, T. A., Zou, J.-Y., Cowan, S. W., and Kjeldgaard, M. (1991) *Acta Crystallogr. A 47*, 110−119.
24. Kukimoto, M., Nishiyama, M., Murphy, M. E., Turley, S., Adman, E. T., Horinouchi, S., and Beppu, T. (1994) *Biochemistry 33*, 5246−5252.
25. Hulse, C. L., Tiedje, J. M., and Averill, B. A. (1988) *Anal. Biochem. 172*, 420−426.
26. Olesen, K., Veselov, A., Zhao, Y., Wang, Y., Danner, B., Scholes, C. P., and Shapleigh, J. P. (1998) *Biochemistry 37*, 6086−6094.
27. Zhao, Y., Lukoyanov, D. A., Toropov, Y. V., Wu, K., Shapleigh, J. P., and Scholes, C. P. (2002) *Biochemistry 41*, 7464−7474.
28. Jeuken, L. J. C., Ubbink, M., Bitter, J. H., van Vliet, P., Meyer-Klaucke, W., and Canters, G. W. (2000) *J. Mol. Biol. 299*, 737−755.
29. Solomon, E. I., Sunduram, U. M., Machonkin, T. E. (1996) *Chem. Rev. 96*, 2563−2605.
30. Guss, J. M., Harrowell, P. R., Murata, M., Norris, V. A., and Freeman, H. C. (1986) *J. Mol. Biol. 192*, 361−387.

31. Vakoufari, E., Wilson, K. S., and Petratos, K. (1994) *FEBS Lett. 347*, 203−206.
32. LaCroix, L. B., Shadle, S. E., Wang, Y. N., Averill, B. A., Hedman, B., Hodgson, K. O., and Solomon, E. I. (1996) *J. Am. Chem. Soc. 118*, 7755−7768.
33. Pierloot, K., De Kerpel, J. O. A., Ryde, U., Olsson, M. H. M., and Roos, B. O. (1998) *J. Am. Chem. Soc. 120*, 13156−13166.
34. Adman, E. T., Godden, J. W., and Turley, S. (1995) *J. Biol. Chem. 270*, 27458−27474.
35. Messerschmidt, A., Prade, L., Kroes, S. J., Sanders-Loehr, J., Huber, R., and Canters, G. W. (1998) *Proc. Natl. Acad. Sci. U.S.A. 95*, 3443−3448.
36. Boulanger, M. J., and Murphy, M. E. (2002) *J. Mol. Biol. 315*, 1111−1127.
37. Guss, J. M., Merritt, E. A., Phizackerley, R. P., and Freeman, H. C. (1996) *J. Mol. Biol. 262*, 686−705.
38. Petratos, K., Dauter, Z., and Wilson, K. S. (1988) *Acta Crystallogr. B 44*, 628−36.
39. Dodd, F. E., Van Beeumen, J., Eady, R. R., and Hasnain, S. S. (1998) *J. Mol. Biol. 282*, 369−382.
40. Inoue, T., Gotowda, M., Deligeer, Kataoka, K,. Yamaguchi, K., Suzuki, S., Watanabe, H., Gohow, M., Kai, Y. (1998) *J. Biochem. 124*, 876−879.
41. Bond, C. S., Blankenship, R. E., Freeman, H. C., Guss, J. M., Maher, M. J., Selvaraj, F. M., Wilce, M. C., and Willingham, K. M. (2001) *J. Mol. Biol. 306*, 47−67.
42. Karlsson, B. G., Tsai, L. C., Nar, H., Sanders-Loehr, J., Bonander, N., Langer, V., and Sjolin, L. (1997) *Biochemistry 36*, 4089−4095.
43. Durley, R., Chen, L., Lim, L. W., Mathews, F. S., and Davidson, V. L. (1993) *Protein Sci. 2*, 739−752.
44. Guss, J. M., Bartunik, H. D., and Freeman, H. C. (1992) *Acta Crystallogr. B 48*, 790−811.
45. Nar, H., Messerschmidt, A., Huber, R., van de Kamp, M., and Canters, G. W. (1991) *J. Mol. Biol. 221*, 765−772.
46. Romero, A., Hoitink, C. W., Nar, H., Huber, R., Messerschmidt, A., and Canters, G. W. (1993) *J. Mol. Biol. 229*, 1007−1021.
47. Murphy, M. E., Turley, S., Kukimoto, M., Nishiyama, M., Horinouchi, S., Sasaki, H., Tanokura, M., and Adman, E. T. (1995) *Biochemistry 34*, 12107−12117.
48. Kobayashi, K., Tagawa, S., Deligeer, and Suzuki, S. (1999) *J. Biochem. (Tokyo) 126*, 408−412.
49. Suzuki, S., Deligeer, Yamaguchi, K., Kataoka, K., Kobayashi, K., Tagawa, S., Kohzuma, T., Shidara, S., and Iwasaki, H. (1997) *J. Biol. Inorg. Chem. 2*, 265−274.
50. Farver, O., Eady, R. R., Abraham, Z. H., and Pecht, I. (1998) *FEBS Lett. 436*, 239−242.

BI027270+